Review

Cancer Research

Mesoscopic and Macroscopic Optoacoustic Imaging of Cancer

Adrian Taruttis[1,2], Gooitzen M. van Dam[1], and Vasilis Ntziachristos[2,3]

Abstract

Optoacoustic imaging combines the rich contrast of optical methods with the resolution of ultrasound imaging. It can therefore deliver optical visualization of cancer far deeper in tissue than optical microscopy and other conventional optical imaging methods. Technological progress and novel contrast media have resulted in optoacoustic imaging being propagated to basic cancer research and in clinical translation projects. We briefly review recent technological advances, showcase the ability to resolve unique cancer biomarkers based on spectral features at different imaging scales, and highlight the imaging performance achieved in preclinical and clinical imaging applications. *Cancer Res; 75(8); 1548–59. ©2015 AACR.*

Introduction

Optical imaging plays a crucial role in cancer research and cancer detection. Optical methods are used in the laboratory to reveal complex biologic processes underpinning cancer through a range of endogenous and exogenous contrast sources. In parallel, optical endoscopy and laparoscopy are widely applied for cancer detection in screening, diagnostic, or therapeutic procedures. However, the use of light for cancer visualization comes with the inherent limitation that strong scattering in tissue causes the degradation of spatial information and quantification after the first few hundred microns below the tissue surface (1). Optoacoustic imaging can overcome this limitation by visualizing optical absorption in tissues using acoustic detection. The tissue is typically illuminated by a short pulse of light (e.g., ~10 ns duration). Visible light propagates for a few millimeters within tissue, whereas light in the near-infrared (NIR) can reach depths of several centimeters (1). At locations within tissue where this light is absorbed, the absorbing material undergoes thermal expansion, giving rise to pressure waves that propagate outwards and can be detected noninvasively by ultrasound transducers. The ultrasound detected is used to reconstruct images of the origin of optical absorption within tissue. Because ultrasound waves scatter orders of magnitude less than light, the detection of optical contrast based on ultrasound instead of light leads to higher spatial resolution beyond the penetration limits of optical microscopy.

Since its original inception in the 1970s (2), optoacoustic imaging has remained largely an experimental technique. Single detector and single wavelength experimental systems demonstrated aspects of biological imaging in the 90s (3, 4), but did not offer features that enabled wide dissemination. However, considerable technical progress in recent years has led to high-quality images and the ability to resolve rich contrast with performance often not available to other imaging methods. Multispectral optoacoustic tomography (MSOT), in particular, provides spectral detection of absorption contrast to visualize a number of cancer-relevant endogenous tissue components, including hemoglobin oxygenation and volume as well as melanin, and a range of exogenous contrast agents, including clinically approved optical dyes [e.g., Indocyanine Green (ICG) and methylene blue (MB)] and novel agents with molecular specificity (5). As a gateway to clinical applications, the implementation of MSOT as a real-time imaging method opens up possibilities in cancer care and in the study of dynamic processes. Furthermore, MSOT is scalable from microscopic views close to the surface to macroscopic imaging of deep tissue (e.g., whole breasts; refs. 1, 6). Importantly, the use of quantitative algorithms for image reconstruction and a new generation of spectral unmixing algorithms not only allow quantitative imaging but also improve the sensitivity of MSOT by at least an order of magnitude over conventional spectral implementations.

Optoacoustic imaging can be generally separated in two classes. The first class, scans a focused beam of pulsed light over tissue and collects the generated sound. Images are formed simply by placing the measurements collected onto a raster corresponding to the scan pattern collected. This approach can provide a high spatial resolution limited by optical diffraction and is referred to as optoacoustic (or photoacoustic) microscopy (6–8). Because the principle of operation relies on focused light, this approach is limited to depths common to other optical microscopy techniques such as multi-photon microscopy (typically the first few hundred microns beneath the illuminated tissue surface).

In this article, we provide a critical analysis of the second class of optoacoustic methods that can be referred to as optoacoustic (or photoacoustic) mesoscopy or macroscopy and enable imaging deeper than optical or optoacoustic microscopy methods that use focused light (1). Images are formed by reconstructing the absorbed energy distribution after sampling time-resolved optoacoustic signals at multiple positions around the region of interest. Because ultrasound attenuation in tissue increases with frequency,

[1]Department of Surgery, University Medical Center Groningen, University of Groningen, Groningen, the Netherlands. [2]Institute for Biological and Medical Imaging, Helmholtz Zentrum München, Neuherberg, Germany. [3]Chair for Biological Imaging, Technische Universität München, Munich, Germany.

Corresponding Author: Vasilis Ntziachristos, Chair for Biological Imaging, Technische Universität München, Ismaningerstr. 22, 81675 München, Germany. Phone: 49-89-31873852; Fax: 49-89-3187173852; E-mail: v.ntziachristos@tum.de

doi: 10.1158/0008-5472.CAN-14-2522

spatial resolution, which depends on ultrasound frequency, can be traded off against penetration depth. Mesoscopy typically refers to depths of a few millimeters (1–5 mm) with the resolution in the order of a few microns to tens of microns. Macroscopy then refers to depths beyond 5 mm and resolution ranging from tens of microns to a few hundred of microns, depending on the depth. Illumination is typically wide-field and the imaging performance depends on the ultrasound detector parameters and their geometry, as well as the image reconstruction algorithms used.

We review recent progress in mesoscopic and macroscopic optoacoustic imaging of cancer, which has not been covered in other reviews of optoacoustic imaging. We showcase advances and unique optoacoustic imaging abilities in resolving cancer biomarkers, enabled by recent innovations in light source technology, real-time detection, and multispectral processing methods. Furthermore, we highlight developments in contrast media relevant to optoacoustic imaging of cancer, including recent nanomedicine platforms. Finally, we show recent experimental studies that have demonstrated the potential for unique preclinical and translational clinical imaging of cancer.

Imaging Performance and Sensitivity Enhancement

Optoacoustic imaging has been primarily based on pulsed lasers in the nanosecond pulse duration range, which deposit sufficient energy within a short time and generate acoustic waves through thermoelastic expansion, while avoiding concurrent thermal diffusion. Optoacoustic images can be generated at single wavelengths and reveal contrast based on light absorption in tissue; the stronger the light absorption in tissue, the larger the intensity of the optoacoustic signal detected. Contrast in tissue is generated by chromophores including hemoglobin, melanin, lipids, and water. These images can be further enhanced using contrast agents that absorb light, including fluorochromes and appropriate nanoparticles (e.g., carbon nanotubes, gold nanoparticles, etc.; refs. 5, 9).

Figure 1 depicts whole-body cross-sectional images through mice showing elaborate anatomic contrast, including vascular structures in the brain (Fig. 1B), the liver, spinal cord, and aorta (Fig. 1C) and the kidneys and spleen (Fig. 1C). Such structures have never been visualized before through whole animals *in vivo* using conventional optical imaging methods.

Four technological advances have made this performance possible:

1. *Ring illumination technology*. As shown in Fig. 1A, which concentrates the available energy along a mouse slice in a diffusive manner. This can be achieved by multiple illumination fibers arranged to direct energy to the mouse in a cylindrical fashion (10).
2. *Acquisition electronics for parallel detection*. Progress in electronics allows multiple optoacoustic signals to be sampled in parallel at up to 125 megasamples/s, enabling the utilization of multiple-element detectors that avoid time-consuming scanning or multiplexing processes (11, 12).
3. *Cylindrically focused detector arrays*. The images in Fig. 1 were generated by a 256-channel detection array that was cylindrically focused to deliver cross-sectional images from mouse slices of approximately 1-mm slice thickness (12). Cylindrical focusing is important to minimize contributions from out of plane signals and reveal images of virtual mouse cross-sections; typically of 0.5- to 1.5-mm thickness.
4. *Advanced reconstruction approaches.* Model-based methods have been developed to offer imaging performance that is superior to simple delay-and-sum or back-projection methods as they can account for the characteristics of the imaging system (13, 14) and can lead to quantitative images (15).

Figure 1B–D were acquired by collecting optoacoustic signals at single detector array positions along the axial dimension, generating transverse images. For each detector position, a corresponding axial image is generated. Alternatively, scans from the entire animal can be reconstructed as a three-dimensional (3D) volume, as shown in Fig. 1E, which depicts contrast from the blood vessels visible from the dorsal side of a mouse (16, 17).

Advances in multispectral detection and sensitivity improvements

Although single wavelength imaging reveals anatomic features, a major advantage of optoacoustic cancer imaging comes from tissue illumination at multiple wavelengths. MSOT uses algorithms referred to as spectral unmixing that can detect the spectra of different molecules of interest present in tissue by analyzing the images obtained at multiple wavelengths. MSOT combines high-resolution morphologic imaging with background-free molecular sensing more typical to nuclear imaging methods, but at a high spatial resolution.

An important feature of spectral unmixing is that it can improve the detection sensitivity of MSOT over conventional (single wavelength) optoacoustic imaging. We have recently demonstrated that excitation at multiple optical wavelengths, combined with a statistical subpixel detection method (adaptive matched filter—AMF) for spectral unmixing (18), can effectively enhance the sensitivity over single wavelength optoacoustic imaging on the order of 14 to 40 times in molecular imaging applications (19). This performance is summarized in Fig. 2, depicting MSOT imaging of a mouse brain with an orthotopic glioblastoma expressing the NIR fluorescent protein iRFP. In particular, Fig. 2B shows an image acquired at the excitation peak of iRFP where no noticeable signal is detected from the target over background. In contrast, spectral unmixing using AMF at 12 wavelengths resolved the iRFP with high contrast over the background, as shown in Fig. 2C. Simplistic approaches such as subtracting an image obtained at a wavelength that is off the absorption maximum of the target chromophore from an image obtained at the absorption maximum do not provide robust or sensitive detection in general, as can be seen in Fig. 2E. This is because there are wavelength-dependent absorption changes of the background tissue as well that affect the subtracted image.

The MSOT sensitivity depends on a number of parameters, such as the depth and volume of the lesion (20), the absorption coefficient of the molecular agent, or the spectral unmixing approach used (18). Although a thorough analysis of the sensitivity capabilities of the technology is yet to be performed, experimental evidence shows detection of approximately 5 pmol of a NIR fluorescent dye in deep tissue in mice (19).

In comparison, fluorescence imaging in deep tissue, such as fluorescence molecular tomography (FMT), is known to have a detection sensitivity on the order of 1 pmol (21). However, these comparisons are so far done on voxels that are one to three orders of magnitude smaller in MSOT. Alternative contrast mechanisms

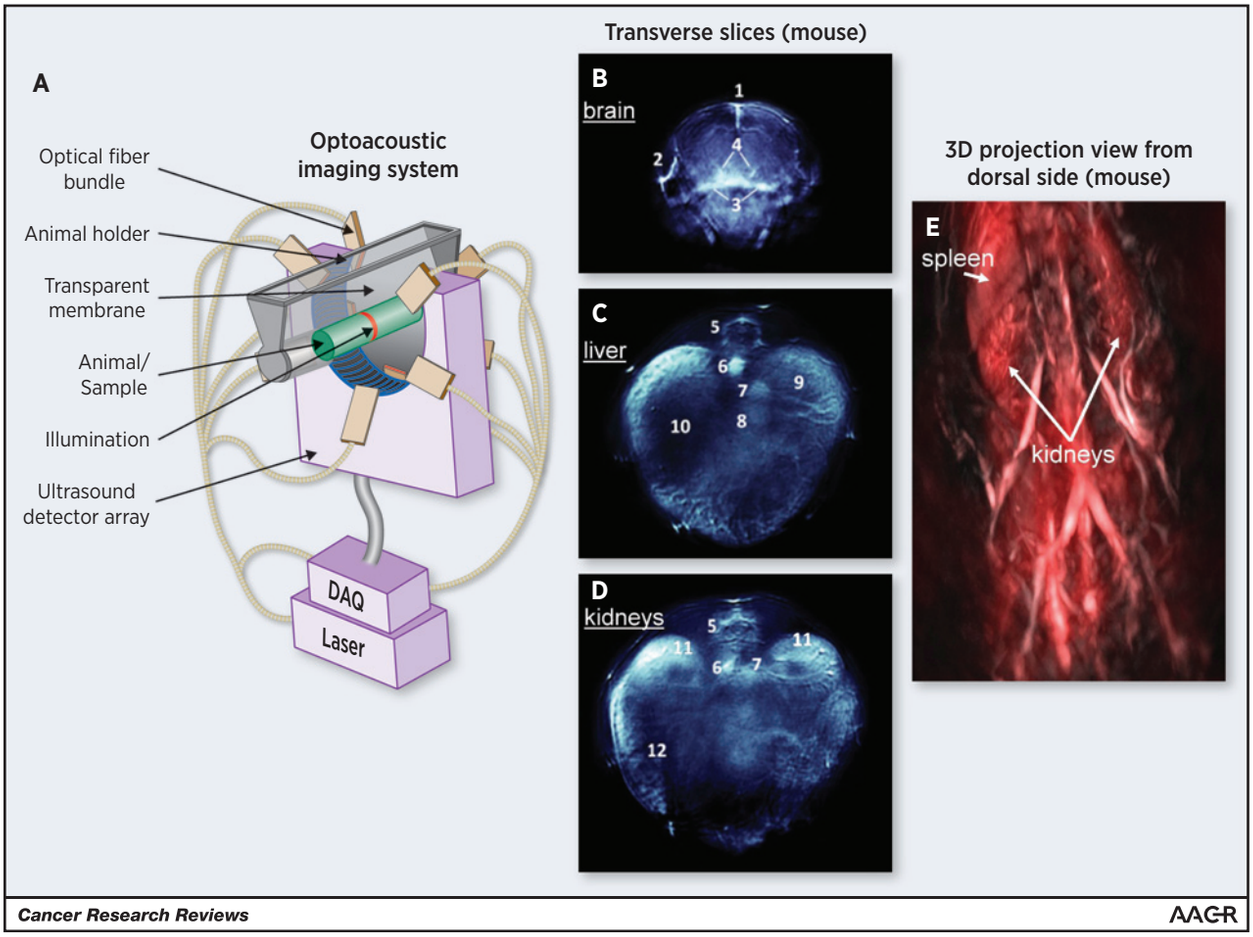

Figure 1.
Optoacoustic imaging. A, a tomographic imaging system for small animals. The animal is held inside a membrane that is transparent to light and ultrasound. Laser pulses excite optoacoustic signals, which are detected by means of an ultrasound transducer array. B–D, optoacoustic slices through a mouse in the transverse plane, showing the brain (B), the liver (C), and the kidneys (D). These images were each captured from a single laser pulse, resulting in an image acquisition times in the tens of microseconds. The following structures were identified: 1, sagittal sinus; 2, temporal artery; 3, extra-cranial blood vessel; 4, deep cerebral vessel; 5, spinal cord; 6, aorta; 7, vena cava; 8, vena porta; 9, liver; 10, stomach; 11, kidney; 12, spleen. The images are reproduced from Dima A, Burton NC, Ntziachristos V. Multispectral optoacoustic tomography at 64, 128, and 256 channels. J Biomed Opt. 2014 March, 19(3):036021 with permission. E, a maximum intensity projection showing a volume of the mouse abdomen, viewed from the dorsal side. The image is reconstructed after rotating a linear ultrasound array around the mouse according to the method described in ref. 16. Image courtesy of Jérôme Gateau.

such as melanin or photo-absorbing nanoparticles may offer two to three orders of magnitude better sensitivity due to their high absorption coefficients (5).

Advances in illumination technology

MSOT gains access to multiple wavelengths by using tunable light sources, including optical parametric oscillators (OPO), Ti: Sapphire lasers, Alexandrite lasers, and dye lasers, all of which have been used in optoacoustic imaging systems in the research environment. MSOT with slow tuning lasers or low pulse repetition rates present several disadvantages. Motion either originating in handheld detectors or the tissue itself may change the volume imaged between wavelengths and lead to spectral unmixing errors (22).

Recent investment and innovations in OPO systems has resulted in sources that are fast-tuning. Systems that use fast mechanical control of the nonlinear optical crystal orientation have been demonstrated to operate at 50 different wavelengths per second in macroscopy applications, providing MSOT at multiple frames per second (e.g., 10 multispectral images per second at 5 wavelengths each; refs. 23, 24). At more superficial depths, that is, in mesoscopic applications, it is possible to operate with lower pulse energy, which allows higher pulse repetition rates, potentially providing frame rates in the kHz range. Finally, the emergence of frequency domain optoacoustic imaging could play a critical role in lowering the cost and complexity of optoacoustic systems (25–27), by replacing pulsed lasers by modulated continuous wave illumination.

Advances in real-time 2D and 3D handheld operation

The recent availability of acquisition electronics to detect optoacoustic signals from multiple detectors in parallel (up to 512 parallel channels reported; ref. 28), and progress with fast tuning light sources (24) has led to breakthrough MSOT implementations that are capable of high-quality real-time imaging. Systems using multi-element ultrasound detector arrays have

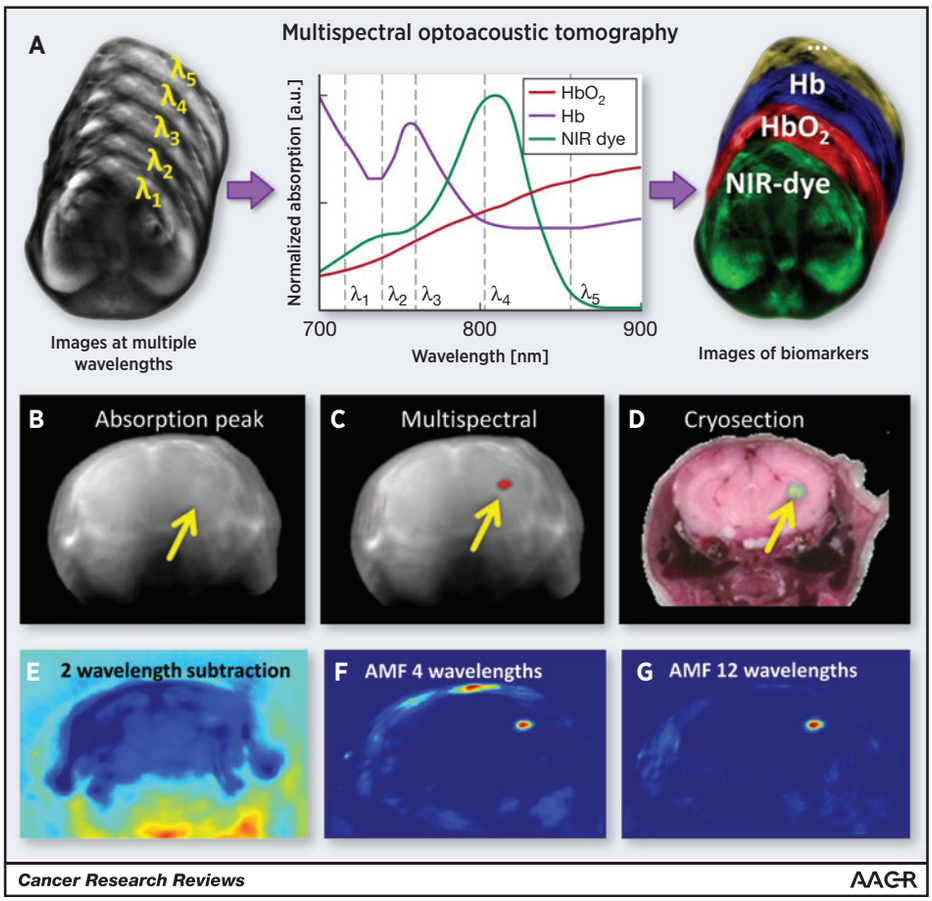

Figure 2.
MSOT resolves optical biomarkers by means of their unique absorption spectra. A, optoacoustic images acquired at multiple wavelengths are input to an appropriate spectral unmixing algorithm together with knowledge of the absorption spectra of target materials. The results are images of each absorber. B and C, imaging at multiple wavelength enhances the detection sensitivity of MSOT. B, an optoacoustic image of a mouse brain bearing a tumor (glioblastoma) expressing the NIR fluorescent protein iRFP is shown. The image was acquired with optical excitation at the absorption peak of iRFP, but the tumor, located at the yellow arrow, is invisible in the image. C, the same image is shown, but with a red overlay of iRFP signal obtained by MSOT using excitation at 12 wavelengths. AMF was used for sensitive spectral unmixing. D, an *ex vivo* cryosection of the same animal validates the location of the tumor, with NIR fluorescence shown in green. E, the result of unmixing by subtracting an image acquired at an off-peak part of the target absorption spectrum from an image acquired at the peak (730 nm and 680 nm, respectively). The tumor signal is far lower than some regions of the background. F, the result of AMF using four wavelengths. G, AMF using 12 wavelengths, as used to produce the overlay in C. B–G are reproduced with permission from Tzoumas S, Nunes A, Deliolanis NC, Ntziachristos V. Effects of multispectral excitation on the sensitivity of molecular optoacoustic imaging. J Biophotonics 2014.

demonstrated not only 2D real-time imaging (29, 30), but also 3D real-time imaging of tissue volumes (28, 31), as also shown in Fig. 6A–E. Real-time handheld MSOT operation in a form similar to diagnostic ultrasound imaging can be considered a crucial step toward clinical applications (32–37), particularly when combined with fast wavelength tuning (24).

Multispectral Contrast, Time, and Cancer Biomarkers

Owing to advances in MSOT technology over the past years, it can now provide multiple channels of information for cancer imaging simultaneously. First, single wavelength imaging (Fig. 1) can be used to visualize vascularization, invasion, and overall morphologic features. Second, physiologic and molecular readings, such as perfusion and oxygenation, can be obtained using spectral techniques in label-free or contrast enhanced modes. Third, time dynamics can be studied. Images acquired in real-time can enable imaging of rapid temporal dynamics, for example, the uptake curves of exogenous agents in specific organs or tissue regions, and therefore characterize the pharmacokinetic and biodistribution profiles of novel therapeutic or imaging agents (38–40). Fourth, because of the broadband optoacoustic signals encode a broad range of image scales, MSOT imaging is typically multiscale, displaying, for example, microvasculature alongside large blood vessels (41). In the following, we discuss contrast generation approaches related to these dimensions to reveal cancer biomarkers.

Endogenous contrast

Hemoglobin—tumor angiogenesis, vascular morphology, and oxygenation status. Hemoglobin is the dominant absorber of light at the visible and NIR wavelengths commonly applied in optical imaging. The optoacoustic contrast resulting from absorption of

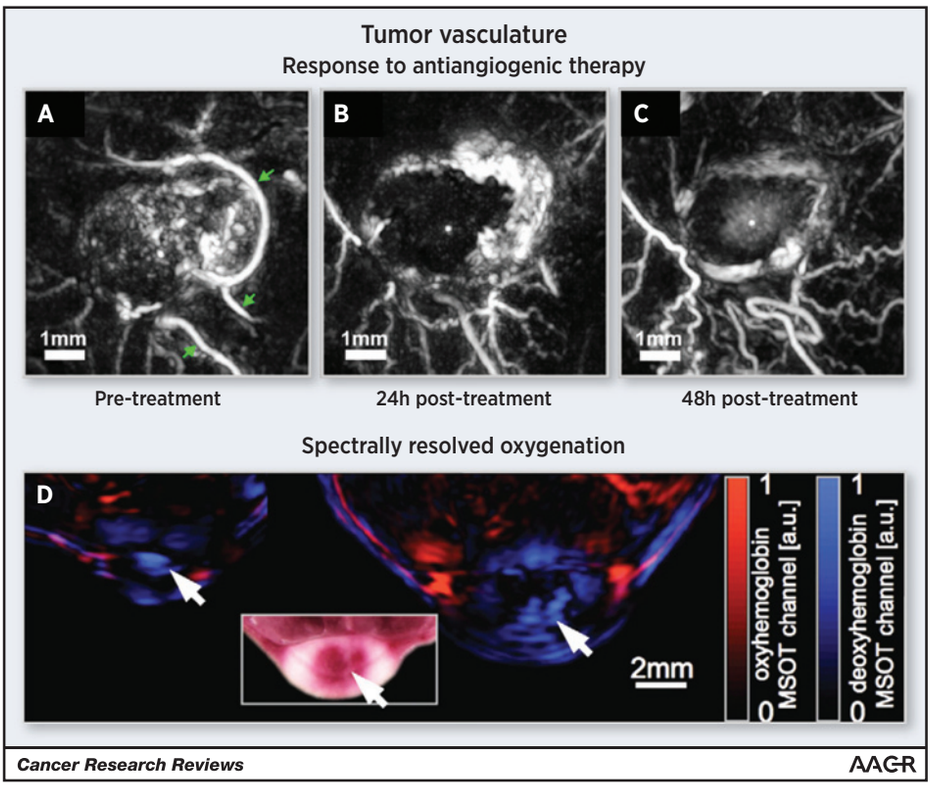

Figure 3.
Optoacoustic imaging of tumor vasculature. A–C, optoacoustic images of tumor vasculature using hemoglobin contrast, showing the effects of a vascular disrupting agent OXi4503 on a xenograft mouse model of human colon carcinoma (cell line LS174T). The images show progression from pretreatment (A), vascular disruption 24 hours after treatment (B), and limited reperfusion after 48 hours (C). A–C are reproduced with permission from Laufer J, Johnson P, Zhang E, Treeby B, Cox B, Pedley B, Beard P. *In vivo* preclinical photoacoustic imaging of tumor vasculature development and therapy. J Biomed Opt 2012 May;17(5):056016. D, multispectral optoacoustic imaging resolving the distributions of oxy- and deoxyhemoglobin within a tumor in a living mouse at two different time points in its development: day 6 (left) and day 13 after inoculation with 4T1 mouse mammary tumor cells. The corresponding *ex vivo* cryosection through the tumor is shown in the inset. D is reproduced with permission from Herzog E, Taruttis A, Beziere N, Lutich AA, Razansky D, Ntziachristos V. Optical imaging of cancer heterogeneity with multispectral optoacoustic tomography. Radiology 2012;263:461–8.

light by hemoglobin allows sensitive imaging of vascular morphology. Figure 3A–C shows images from a study where the response of tumor vasculature to a vascular disrupting agent was imaged, depicting in detail the torturous blood vessels resulting from tumor angiogenesis (42). Using MSOT, it is furthermore possible to distinguish between the oxygenation states of hemoglobin, producing spatial maps of blood oxygen saturation within vessels and perfused tissue (29, 43), as shown for tumor-bearing mice in Fig. 3D. Hemoglobin imaging has been considered in applications related to cancer for tumor detection and characterization in the context of breast cancer (44), oral cancer (45), and prostate cancer (46), resolving vascular abnormalities and oxygenation status (29, 47), and characterizing the response to antiangiogenic agents (42, 48).

Melanin—melanoma metastasis. A further prominent source of endogenous contrast for cancer imaging is melanin, which displays absorption over a broad range of wavelengths in the visible and NIR, decreasing at longer wavelengths. Optoacoustic imaging of melanin has been investigated to assess melanoma depth ingrowth (7) and lymph node staging (49, 50). Its ability to detect circulating melanoma cells has been also reported (51). Detection of melanin originating from melanoma metastases in human lymph nodes imaged after resection is shown in Fig. 4A and B.

Other endogenous absorbers. Several other endogenous tissue absorbers can be detected by illuminating them at the appropriate wavelength, although they may not all have direct relevance to cancer. Lipids have been imaged at NIR wavelengths (52, 53). Water provides strong absorption at NIR wavelengths longer than 900 nm (54). Bilirubin imaging has been demonstrated at blue wavelengths (55) as has imaging of cytochromes (56); however, limited penetration depth in this region of the spectrum limits their applicability. Finally, label-free imaging of cell nuclei by means of DNA and RNA absorption of UV light has also been reported (57), although clinical less relevant.

Exogenous contrast

Exogenous contrast can be provided by agents with sufficient optical absorption to allow optoacoustic detection. Absorption at NIR wavelengths in the 700 to 900 nm range is particularly useful because light attenuation in tissue is lower at those wavelengths than in the visible, providing increased penetration depth. Such agents should also display absorption spectra that are distinct from endogenous tissue chromophores, so that they

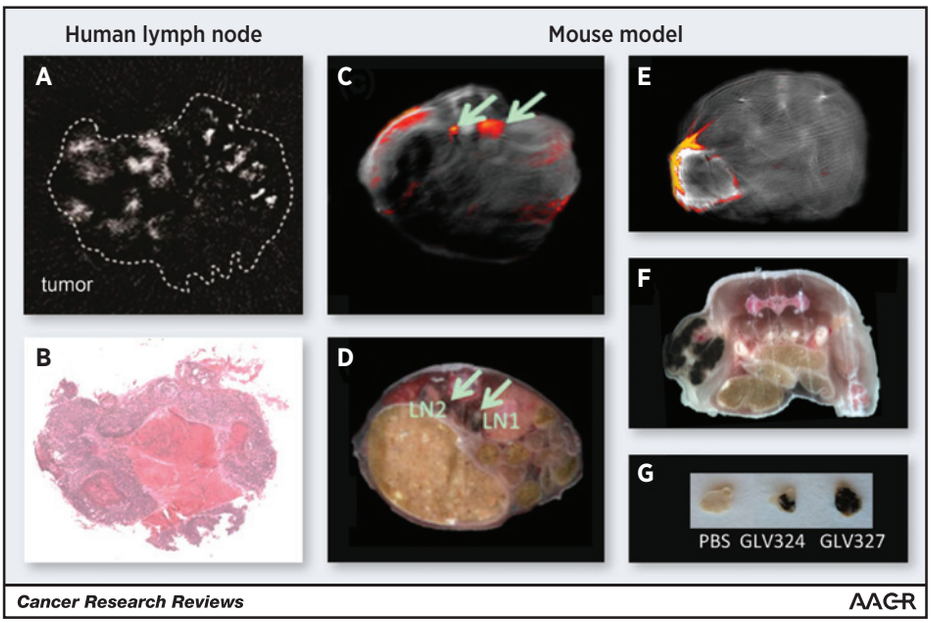

Figure 4.
Optoacoustic imaging of endogenous and transgenically expressed melanin. A, resected lymph node with melanoma metastasis. The white spots correspond to increased optoacoustic signal originating from melanin. B, corresponding H&E stain. A and B are reproduced with permission from Jose J, Grootendorst DJ, Vijn TW, et al., Initial results of imaging melanoma metastasis in resected human lymph nodes using photoacoustic computed tomography. J Biomed Opt 2011 Sep;16(9):096012. C and D show a multispectral optoacoustic image and the corresponding cryosection of a mouse model of cancer (prostate cancer cell line PC-3) after injection with a vaccinia virus that mediates melanin production. The arrows show lymph node metastases (LN1 and LN2) that produce detectable melanin contrast. E and F, the population of a tumor site by the vaccinia virus mediating melanin production. E, an *in vivo* cross-sectional MSOT image of a mouse; color indicates the unmixed melanin spectrum (F) corresponding cryoslice. G, excised tumors from a control animal (PBS) as well as the viral strains GLV-1h324 and GLV-1h327, showing melanin production (black). C and G are reproduced from ref. 74, Copyright 2013 National Academy of Sciences, USA.

can be separated from the tissue background by spectral unmixing. Different contrast generation strategies have been proposed for optoacoustic imaging; here, we summarize methods and describe their potential for laboratory or clinical use.

Organic dyes and targeted agents. Optoacoustic absorption contrast can be provided by commonly available organic dyes. Prominent examples of clinically available dyes for optoacoustic contrast generation are ICG and MB; however, these are not target-specific and thus only appropriate for perfusion and physiologic imaging. They have been investigated preclinically for lymphatic mapping using optoacoustic imaging by monitoring their uptake in lymph vessels and nodes (58). Photosensitizers, such as zinc phthalocyanine and protoporphyrin IX, which are used clinically for photodynamic therapy (PDT), have also been demonstrated to be detectable to MSOT, allowing their pharmacokinetic and biodistribution profiles to be characterized *in vivo* (Fig. 5G; ref. 40).

Target-specific agents combining a dye with a targeting ligand have been described for optical fluorescence imaging (59) and can be also used in MSOT by capturing the absorption spectrum of the tag. Such agents have been used in MSOT animal studies, for example, to visualize integrins in tumors (43). Organic dyes can also be used in activatable agents, which display changes in their absorption spectra when cleaved by specific enzymes. This mechanism has been used to resolve matrix metalloproteinase (MMP) activity in a mouse model of thyroid cancer (Fig. 5E and F; ref. 60). Dye labels can be added to a wide range of other agents to make them visible to MSOT, including tumor-penetrating dendrimers proposed for therapeutic purposes (61). Agents based on organic dyes have the advantage that they are generally well-characterized because of their wider use in fluorescence imaging. Typical fluorochromes in the NIR display a low quantum yield (fluorescence efficiency) and therefore reserve a large portion of the energy they absorb for optoacoustic signal generation. Use of fluorescence dyes also allows optoacoustic correlation with fluorescence imaging, for example, after tumor removal in a surgical procedure for purposes of detecting microscopic residual disease in positive margins.

Nanoparticles. In addition to organic dyes developed for optical imaging, there is a rapidly growing toolbox of light-absorbing nanoparticles. Different materials that absorb light, such as gold or silver nanoparticles, carbon nanotubes, or iron-oxide particles, have been investigated in optoacoustic imaging studies on animals. Nanoparticles offer promising characteristics over organic dyes in terms of their absorption and photostability and offer an interesting alternative for optoacoustic contrast generation.

Gold nanoparticles (62, 63) have been shown to generate strong optoacoustic signals due to plasmon resonance and can offer a tunable absorption spectrum based on their shape. Imaging of gold nanorods (GNR) and tumor accumulation due to enhanced permeability and retention (EPR) has been demonstrated in Fig. 5H (29), whereas gold nanospheres conjugated to anti-epidermal growth factor receptor (anti-EGFR) have been investigated in the context of tumor targeting

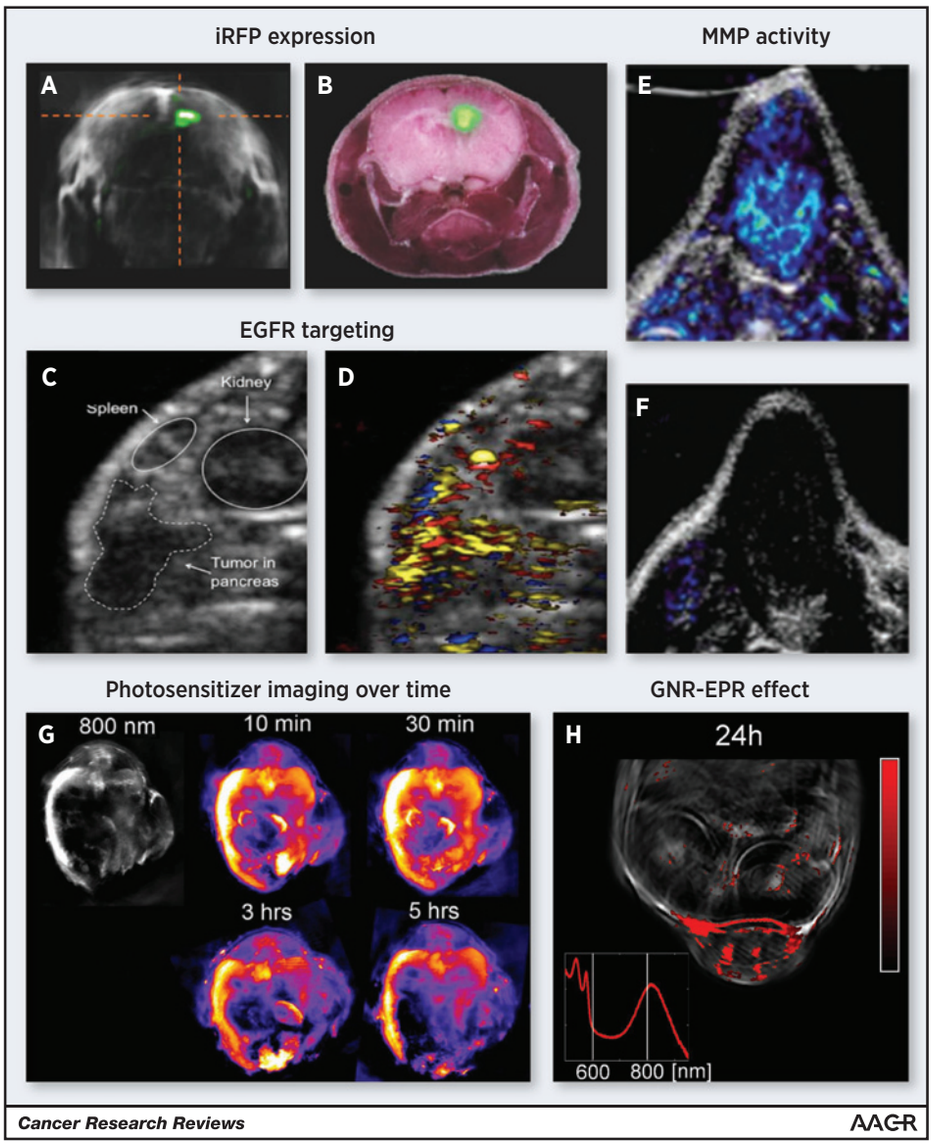

Figure 5.
Optoacoustic imaging of cancer-relevant exogenous contrast agents. A, multispectral optoacoustic imaging of infrared fluorescent protein (iRFP) expression in orthotopic mouse model of glioblastoma (U-87 human glioblastoma cells). Green, iRFP expression. The grayscale background is optoacoustic endogenous tissue contrast. B, corresponding *ex vivo* cryosection photograph showing fluorescence signal from iRFP in green. C and D, targeting of EGFR in an orthotopic mouse model of pancreatic cancer (L3.6pl cells) using a silver nanoplate-anti-EGFR agent. C, a labeled ultrasound image of the region of interest. D, the detected multispectral optoacoustic signals overlaid in yellow (silver nanoplate-anti-EGFR), red (oxyhemoglobin), and blue (deoxyhemoglobin). E and F, imaging of MMP activity in a thyroid carcinoma xenograft in mice using an agent that releases organic dye on cleavage by MMP. E, the activated agent in blue, overlaid on a grayscale ultrasound image of the tumor. F, a control agent for comparison. G, imaging of zinc phthalocyanine photosensitizer over time in a tumor bearing mouse. The grayscale image is taken at 800 nm, while the color images show the photosensitizer detected by MSOT. Signal is visible in the liver, kidneys, spleen, intestines, and tumor xenograft, which is on the right side of the images. H, imaging of EPR in a tumor using long-circulating GNRs. The inset shows the absorption spectrum of a blood sample from the mouse, including the NIR absorption peak of the nanorods. A and B are reproduced from ref. 71, with kind permission from Springer Science and Business Media. C and D are reproduced from ref. 65, reprinted with permission from Homan KA, Souza M, Truby R, Luke GP, Green C, Vreeland E, et al. Silver nanoplate contrast agents for *in vivo* molecular photoacoustic imaging. ACS Nano 2012;6:641–50. Copyright 2015 ACS. E and F are reproduced from ref. 60. G is reprinted by permission from Macmillian Publishers Ltd: Scientific Reports. Ho CJH, Balasundaram G, Driessen W, McLaren R, Wong CL, Dinish US, et al. Multifunctional photosensitizer-based contrast agents for photoacoustic imaging. Sci Rep 2014;4:5342. H is reproduced with permission from Herzog E, Taruttis A, Beziere N, Lutich AA, Razansky D, Ntziachristos V. Optical imaging of cancer heterogeneity with multispectral optoacoustic tomography. Radiology 2012;263:461-8.

(63). Further salient examples include *in vivo* brain tumor contrast enhancement by gold nanospheres coated with gadolinium and a Raman-molecular tag to enable trimodal visualization by MRI, optoacoustics, and Raman imaging (64). Silver nanoplates with absorption peaks around 800 nm functionalized with antibodies for EGFR targeting (65) have been also

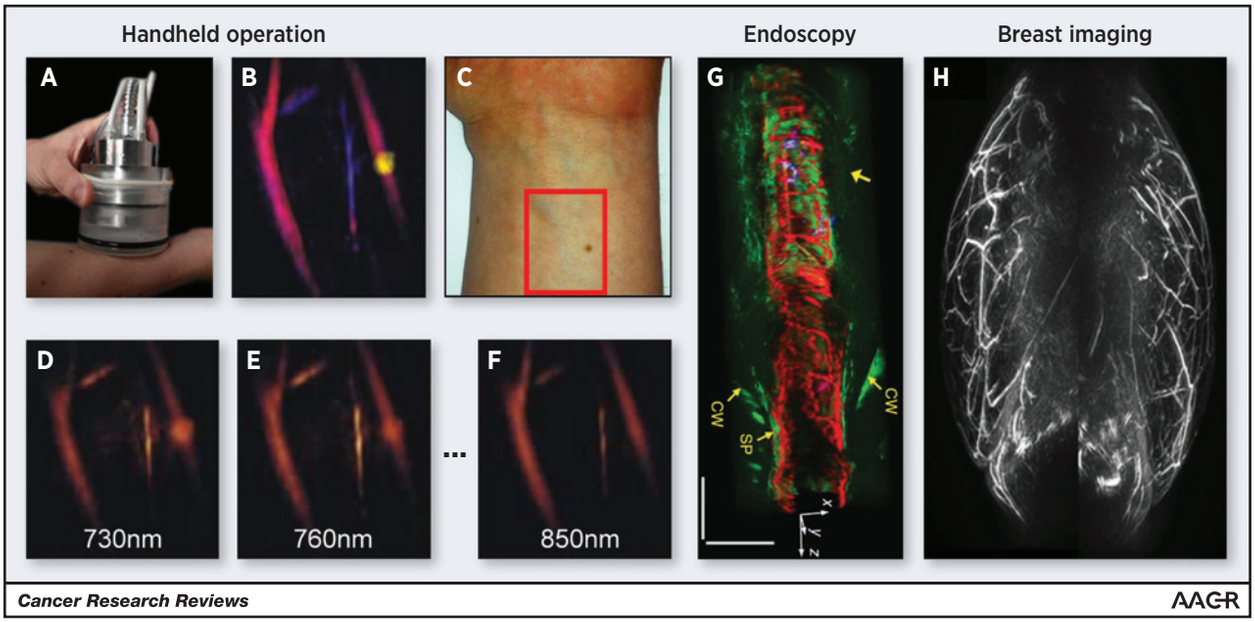

Figure 6.
Optoacoustic imaging implementations with clinical relevance. A, a handheld 3D real-time MSOT system. B, multispectral optoacoustic image of the forearm simultaneously resolving veins (blue), arteries (red), and superficial melanin (yellow). The image is a maximum intensity projection of a 3D dataset and is generated by spectral unmixing of images acquired in multiple wavelengths D–F. C, a photograph of the arm showing the imaged region (red box). G, combined optoacoustic and ultrasound endoscopy of the colon and surrounding tissue in a rat (81). Red, vasculature; blue, lymph nodes and vessels highlighted by Evans Blue dye; green, ultrasound image. H, 3D breast imaging using dedicated scanner. The subject is a healthy volunteer with DD cup size. Vasculature is visible throughout the breast. A–F are reprinted by permission from Macmillan Publishers Ltd: Light:Science and Applications. Luís Dean-Ben X, Razansky D. Adding fifth dimension to optoacoustic imaging: volumetric time-resolved spectrally enriched tomography. Light Sci Appl 2014:3:e137. Copyright 2014. G is reprinted by permission from Macmillian Publishers Ltd: Nature Medicine, Yang J-M, Favazza C, Chen R, Yao J, Cai X, Maslov K, et al. Simultaneous functional photoacoustic and ultrasonic endoscopy of internal organs *in vivo*. Nat Med 2012;18:1297–1302. Copyright 2012. H is reproduced from ref. 81, with permission from AAPM.

considered to image pancreatic cancer, as shown in Fig. 5C and D. Liquid perfluorocarbon nanodroplet vaporization, using encapsulated plasmonic nanoparticles to generate absorption, has also been investigated for optoacoustic contrast (66). In addition, single-walled carbon nanotubes also produce optoacoustic signals and they have been conjugated to cyclic Arg–Gly–Asp peptides (RGD) for tumor targeting in mice (67). Nanoparticle-based activatable agents can be developed for optoacoustic imaging. An agent based on a combination of copper sulfide and a quencher that can be separated by MMP activity, thus altering the absorption spectrum, has been reported in the context of mouse tumor models (68).

Iron oxide nanoparticles have also been investigated for optoacoustic imaging. Several forms of iron oxide nanoparticles have the advantage of clinical approval for use as MRI contrast agents. In particular, superparamagnetic iron oxide nanoparticles (SPIO) were studied as agents for lymph node staging in a rat model of prostate cancer, where the lack of uptake in metastases compared with healthy tissue provided negative optoacoustic image contrast in specimens imaged *ex vivo* (69). HER-2/neu–targeted iron oxide nanoparticles have been investigated for imaging of ovarian cancer in a mouse model (70). However, iron oxide particles typically do not display high optical absorption in the NIR, which makes *in vivo* detection highly challenging.

Generally, novel nanoparticles offer promising characteristics for optoacoustic signal generation. A caveat for clinical use is that novel nanoparticles have to gain regulatory approval before human use, as certainty about safety must be established for each individual type of nanoparticle, which may slow their dissemination ability.

Transgenic technologies. Although fluorescent proteins are restricted to laboratory use, they comprise a powerful tool for cancer research and can also be visualized by optoacoustic imaging. In particular, recently developed NIR fluorescent proteins allow imaging with deep tissue penetration (71, 72). Figure 5A and B shows detection of iRFP, a NIR fluorescent protein, being expressed by glioblastoma cells in the mouse brain.

An exciting recent development is the consideration of alternative transgenic technologies for cancer imaging based on melanin production, which is better suited for strong optoacoustic signal generation (73). Gene-evoked melanin production mediated by an oncolytic Vaccinia virus has been demonstrated for optoacoustic detection of metastases, as can be seen in Fig. 4C–G where melanin is detected in lymph node metastases as well as primary tumors in a mouse model (74). Melanin can also be visualized by MRI, making it a powerful alternative to fluorescent proteins for deep-tissue imaging of reporter genes; furthermore, it can be used for laser-induced thermotherapy by means of the strong absorption of light by melanin (74).

Clinical Cancer Imaging

Because of its spatial, spectral, real-time, and multiscale abilities, optoacoustic imaging can play a role into the clinical

imaging and management of cancer. Two strong differentiation points of MSOT compared with other radiologic modalities are (i) the unique contrast imparted by spectral unmixing, leading to label-free oxy- and deoxyhemoglobin imaging as well as melanin and other tissue chromophores, and (ii) the high-resolution highly scalable molecular imaging capacity. In the following, we review pertinent optoacoustic studies performed on humans or animal studies that showcase the clinical potential of optoacoustic imaging. This review is not an exhaustive account of all studies but rather a window into the versatility of optoacoustic cancer imaging.

Noninvasive breast cancer imaging

Breast cancer has been the focus of several optoacoustic studies. One of the key biomarkers targeted is increased vascular density and the corresponding hemoglobin concentration assumed in breast malignancies. The human breast has low vascular density and generally offers lower attenuation to propagating light, compared with other human tissues. It has been shown that the entire human breast can be generally imaged by optoacoustic imaging in the NIR (28), as shown in Fig. 6G. Imaging of hemoglobin contrast has been performed in pilot studies including 13, 25, and 17 patients with suspected breast cancer respectively (75–77). The most recent of those studies was able to distinguish between malignancies and cysts in all successfully imaged cases (10 patients with malignancies and with two cysts; ref. 77). Each of these studies had technological shortcomings related to their pioneering nature in comparison with the real-time multispectral optoacoustic imaging possible today. In particular, the images were acquired at a single optical wavelength, therefore forgoing the ability to quantify specific physiologic biomarkers of disease (e.g., deoxygenated hemoglobin). In addition, the implementation of fast or real-time MSOT methods may offer better feedback in localizing and characterizing a breast lesion and could also enable handheld operation. Despite their limitations, these studies point to optoacoustic imaging as an alternative mammographic method. There are two gaps in current breast cancer imaging that optoacoustics aims to address. The first is the lack of sensitivity provided by mammography in dense breast tissue. Optoacoustic imaging could provide a modality that misses fewer malignancies in dense breast tissue compared with standard mammography. The sensitivity of X-ray mammography of dense breasts containing high amounts of fibroglandular tissue ranges from 45% (extremely dense) to 70% (heterogeneously dense; ref. 78). In comparison, optoacoustic contrast is not affected by breast density (77). The second gap is the low specificity of ultrasound imaging. By using spectral specificity, MSOT could reveal tissue and cancer biomarkers not available to X-ray mammography or ultrasound. Optoacoustic contrast, if added to ultrasound imaging, could better distinguish between benign lesions and malignancies.

Imaging of the skin

Optoacoustic imaging of the skin can be implemented at a high resolution by increasing the ultrasound detection frequency, providing views of small structures in a reduced field of view with a reduced penetration depth (79). High-resolution systems are suitable for imaging skin lesions, including their vasculature and melanin content (80), as well as any biomarkers available from exogenous agents. Figure 6A–E shows the handheld probe of an MSOT system, which uses a two-dimensional (2D) ultrasound array detector to produce 3D spectral images of the dermis and subcutis in real-time. The system can unmix the contributions of lesions containing melanin and the underlying arteries and veins (23).

Endoscopy

The light delivery and ultrasound detection required for optoacoustic imaging can be miniaturized to enable endoscopic systems for laparoscopic and endoscopic applications. Using such an approach, combined optoacoustic and ultrasound endoscopic imaging of the esophagus and colon has been recently demonstrated in rats and rabbits (81). The resulting optoacoustic images, an example of which is shown in Fig. 6F, displayed vasculature that was invisible to ultrasound, and multispectral information allowed hemoglobin oxygenation as well as an exogenous dye (Evans Blue) in the lymphatic system to be resolved. A further miniaturized endoscopic probe has been developed with a 2.5-mm diameter, allowing it to be inserted into the instrument channel of a standard video endoscope (82). With these technological advances, it is expected that optoacoustic imaging of the gastrointestinal tract will be investigated in patients in the near future. Optoacoustic imaging can reveal depth information of suspicious lesions so that they can be characterized in three dimensions. In addition, characterization of the microvasculature as well as biological targets highlighted by exogenous agents has the potential to provide a more complete picture of imaged lesions than possible by white light endoscopy and confocal endomicroscopy.

Intraoperative imaging

Optoacoustic imaging can address a number of problems in current surgery by providing real-time visualization of optical contrast beyond the tissue surface. The imaging systems are typically sufficiently compact and portable to be brought into the operating room and can provide images rapidly and conveniently, in a manner similar to intraoperative ultrasound (24). Optoacoustic imaging could assess the perfusion status of tissue by detecting hemoglobin dynamics and oxygenation, potentially providing better prediction of anastomotic leakage resulting from ischemic conditions in the colon or esophagus while it can still be prevented (83).

Lymphatic mapping for staging purposes and clinical decision making in surgical oncology can also be addressed by optical and optoacoustic imaging. In current practice, the sentinel node, that is, the first draining lymph node off-stream of the tumor is identified by injection around the tumor of a gamma-emitting radiotracer and a blue dye. The identified node(-s) can be harvested by a minimally invasive procedure and subsequently be sent to pathology for examination of tumor involvement and therefore staging. Recent literature describes the clinical investigation of ICG fluorescence detection for lymphatic mapping as a compliment or replacement for the current radiotracer and blue dye use (84). The optoacoustic method can also be used in this context, addressing the limitations of fluorescence imaging, which only offers 2D surface images and is strongly affected by tissue scattering for deeper-seated lymph nodes. Although the high acceptance and sensitivity of the radiotracer/gamma probe method may hinder the translation of new methods, the potential elimination of

ionizing radiation by optical imaging is attractive and can simplify procedures and safety concerns involved in the intraoperative use of radioactivity. Optoacoustic lymphatic mapping using clinically approved ICG and MB or novel agents has been shown in rats (58, 85, 86) and imaging systems capable of detection at depths of 5 cm have been reported previously (36). For melanoma staging, lymph node metastases, which commonly display a high melanin content, can be intrinsically detected in optoacoustic images (see Fig. 4A; refs. 49, 50, 87).

Optoacoustic imaging of tumor margins based on exogenous contrast has also been considered: a combined approach using optoacoustic imaging initially to assess the depth of tumor followed by fluorescence imaging during resection has been investigated using fluorescence-labeled iron-oxide particles in a mouse model of breast cancer (88).

Discussion

Optical imaging is experiencing a surge in clinical research interest because it has become clear that methods used in basic research, such as fluorescence microscopy, can also play an important role in clinical imaging for purposes of staging, therapeutic monitoring, and image-guided surgery. Recent studies applying fluorescence molecular imaging in endoscopy and surgery of cancer show much promise (89, 90). However, it is clear that purely optical imaging, which is restricted by optical scattering to producing sharp images within only a few hundred microns of the illuminated tissue surface, can access only a small fraction of the human body. The emergence of optoacoustic imaging as a method to produce high-resolution images beyond the scattering barrier promises to extend the reach of optical contrast to larger organs and deeper-seated tumors.

Optoacoustic image contrast can be provided by endogenous tissue absorbers, including hemoglobin and melanin, as well as light-absorbing dyes and nanoparticles that can provide target specificity. We expect that clinical studies involving optoacoustic imaging will initially remain focused on the detection of endogenous contrast, for example, hemoglobin in breast cancer and melanin in melanoma, both because these methods have clinical potential and because they are simpler from a regulatory point of view. However, as has been the case with optical imaging, contrast agents with specificity to biologic targets relevant to cancer will gradually become available for experimental use in humans.

Optoacoustic imaging technology is not yet fully matured and there is therefore a large variety in the system implementations. For optimal translational imaging of cancer, however, it is important that optoacoustic imaging is implemented in such a way that it can be used reliably and provides robust results. We recommend that real-time optoacoustic imaging, or at least systems with short acquisition times are used, so that users have immediate feedback and are able to control the field of view in a manner similar to diagnostic ultrasound imaging. The utilization of fast or real-time systems also allows visualization of rapid changes in tissue, for example, the uptake of exogenous agents. Furthermore, multispectral systems that use multiple optical wavelengths and uniquely identify absorbers by means of their absorption spectra should be used to maximize detection sensitivity and to avoid ambiguity in results because of the intrinsic and unavoidable presence of many different absorbers of light in tissue. There is a wide variety of optoacoustic configurations that can contribute to cancer imaging, including dedicated breast imagers, handheld probes similar to those used in ultrasound imaging, and optoacoustic endoscopes for imaging the gastrointestinal tract.

There are limitations associated with optoacoustic imaging of cancer. In relation to the physical problem of optoacoustic signal generation, the penetration depth is ultimately limited by the penetration depth of the excitation light. NIR light can penetrate multiple centimeters and still generate detectable optoacoustic signals, but penetrating tens of centimeters is unlikely. In addition, optoacoustic imaging is limited to tissue that allows sufficient ultrasound propagation, similar to ultrasound imaging. Imaging of the lungs or through thick bones is highly challenging because of ultrasound propagation mismatches. Imaging of lung cancer and noninvasive imaging of brain tumors in humans appears unlikely to work without at least severe degradation of image quality. Quantification of absorber concentrations in optoacoustic images is considered an unsolved problem, because the wavelength-dependence of light attenuation in tissue distorts the measured optoacoustic spectrum for deep-lying sources (18, 91). With time, optoacoustic imaging systems are likely to become more robust and user-friendly as the technology becomes more established. Much of the preclinical research conducted in the field of optoacoustic imaging has used exogenous imaging agents, which have yet to be approved for use in humans. In particular, novel plasmonic nanoparticles, which are highly promising because the strong light absorption they offer, are unavailable for use in patients. This somewhat limits the molecular imaging capability of optoacoustic imaging, at least until further agents are approved.

We observe that activities in optical imaging of cancer with molecular specificity are increasing, particularly as novel fluorescently tagged targeting ligands (e.g., antibodies or short peptide sequences) are developed and approved for experimental use in humans. As the technology matures, we expect optoacoustic tumor-targeted imaging in humans to be investigated, in addition to the potential that has already been demonstrated in imaging endogenous tissue absorbers including hemoglobin and melanin. Following the trends that have been outlined in this review, noninvasive imaging of the breast, lymph nodes, and the skin, as well as endoscopic imaging of the gastrointestinal tract are the most likely applications of optoacoustic visualization of cancer to be investigated in clinical trials in the near future.

Disclosure of Potential Conflicts of Interest

V. Ntziachristos is a consultant/advisory board member of iThera Medical GmbH and SurgVision SV. No potential conflicts of interest were disclosed by the other authors.

Grant Support

A. Taruttis was supported by a Research Fellowship from the Deutsche Forschungsgemeinschaft (DFG). The work of V. Ntziachristos was supported by an ERC Advanced Grant (233161), the Deutsche Forschungsgemeinschaft (DFG) Sonderforschungsbereich-824 (SFB-824) subproject A1, and the European Union project FAMOS (FP7 ICT, Contract 317744).

Received August 26, 2014; revised December 16, 2014; accepted January 8, 2015; published OnlineFirst April 2, 2015.

References

1. Ntziachristos V. Going deeper than microscopy: the optical imaging frontier in biology. Nat Methods 2010;7:603–14.
2. Wong YH, Thomas RL, Hawkins GF. Surface and subsurface structure of solids by laser photoacoustic spectroscopy. Appl Phys Lett 1978;32:538–9.
3. Kruger RA. Photoacoustic ultrasound. Med Phys 1994;21:127–31.
4. Oraevsky AA, Jacques SL, Esenaliev RO, Tittel FK. Laser-based optoacoustic imaging in biological tissues. Society of Photo-Optical Instrumentation Engineers (SPIE) Conference Series 1994;2134:122.
5. Ntziachristos V, Razansky D. Molecular imaging by means of multispectral optoacoustic tomography (MSOT). Chem Rev 2010;110:2783–94.
6. Wang LV, Hu S. Photoacoustic tomography: *in vivo* imaging from organelles to organs. Science 2012;335:1458–62.
7. Zhang HF, Maslov K, Stoica G, Wang LV. Functional photoacoustic microscopy for high-resolution and noninvasive *in vivo* imaging. Nat Biotechnol 2006;24:848–51.
8. Hu S, Maslov K, Wang LV. Second-generation optical-resolution photoacoustic microscopy with improved sensitivity and speed. Opt Lett 2011; 36:1134–6.
9. Luke GP, Yeager D, Emelianov SY. Biomedical applications of photoacoustic imaging with exogenous contrast agents. Ann Biomed Eng 2012; 40:422–37.
10. Taruttis A, Herzog E, Razansky D, Ntziachristos V. Real-time imaging of cardiovascular dynamics and circulating gold nanorods with multispectral optoacoustic tomography. Opt Express 2010;18:19592–602.
11. Gateau J, Chekkoury A, Ntziachristos V. Ultra-wideband three-dimensional optoacoustic tomography. Opt Lett 2013;38:4671–4.
12. Dima A, Burton NC, Ntziachristos V. Multispectral optoacoustic tomography at 64, 128, and 256 channels. J Biomed Opt 2014;19:36021.
13. Rosenthal A, Ntziachristos V, Razansky D. Model-based optoacoustic inversion with arbitrary-shape detectors. Med Phys 2011;38:4285–95.
14. Queirós D, Déan-Ben XL, Buehler A, Razansky D, Rosenthal A, Ntziachristos V. Modeling the shape of cylindrically focused transducers in three-dimensional optoacoustic tomography. J Biomed Opt 2013;18: 076014.
15. Rosenthal A, Razansky D, Ntziachristos V. Fast semi-analytical model-based acoustic inversion for quantitative optoacoustic tomography. IEEE Trans Med Imaging 2010;29:1275–85.
16. Gateau J, Caballero MAA, Dima A, Ntziachristos V. Three-dimensional optoacoustic tomography using a conventional ultrasound linear detector array: whole-body tomographic system for small animals. Med Phys 2013;40:013302.
17. Brecht H-P, Su R, Fronheiser M, Ermilov SA, Conjusteau A, Oraevsky AA. Whole-body three-dimensional optoacoustic tomography system for small animals. J Biomed Opt 2009;14:064007.
18. Tzoumas S, Deliolanis N, Morscher S, Ntziachristos V. Un-mixing Molecular Agents from Absorbing Tissue in Multispectral Optoacoustic Tomography. IEEE Trans Med Imaging 2013;33:48–60.
19. Tzoumas S, Nunes A, Deliolanis NC, Ntziachristos V. Effects of multispectral excitation on the sensitivity of molecular optoacoustic imaging. J Biophotonics. Oct 2014. [Epub ahead of print].
20. Razansky D, Baeten J, Ntziachristos V. Sensitivity of molecular target detection by multispectral optoacoustic tomography (MSOT). Med Phys 2009;36:939–45.
21. Klohs J, Steinbrink J, Nierhaus T, Bourayou R, Lindauer U, Bahmani P, et al. Noninvasive near-infrared imaging of fluorochromes within the brain of live mice: an *in vivo* phantom study. Mol Imaging 2006;5:180–7.
22. Taruttis A, Claussen J, Razansky D, Ntziachristos V. Motion clustering for deblurring multispectral optoacoustic tomography images of the mouse heart. J Biomed Opt 2012;17:016009.
23. Luís Deán-Ben X, Razansky D. Adding fifth dimension to optoacoustic imaging: volumetric time-resolved spectrally enriched tomography. Light Sci Appl 2014:3:e137.
24. Buehler A, Kacprowicz M, Taruttis A, Ntziachristos V. Real-time handheld multispectral optoacoustic imaging. Opt Lett 2013;38:1404–6.
25. Telenkov S, Alwi R, Mandelis A, Worthington A. Frequency-domain photoacoustic phased array probe for biomedical imaging applications. Opt Lett 2011;36:4560–2.
26. Kellnberger S, Deliolanis NC, Queirós D, Sergiadis G, Ntziachristos V. *In vivo* frequency domain optoacoustic tomography. Opt Lett 2012;37: 3423–5.
27. Mohajerani P, Kellnberger S, Ntziachristos V. Frequency domain optoacoustic tomography using amplitude and phase. Photoacoustics 2014;2: 111–8.
28. Kruger RA, Kuzmiak CM, Lam RB, Reinecke DR, Del Rio SP, Steed D. Dedicated 3D photoacoustic breast imaging. Med Phys 2013;40:113301.
29. Herzog E, Taruttis A, Beziere N, Lutich AA, Razansky D, Ntziachristos V. Optical imaging of cancer heterogeneity with multispectral optoacoustic tomography. Radiology 2012;263:461–8.
30. Xia J, Chatni MR, Maslov K, Guo Z, Wang K, Anastasio M, et al. Whole-body ring-shaped confocal photoacoustic computed tomography of small animals *in vivo*. J Biomed Opt 2012;17:050506.
31. Dean-Ben XL, Ozbek A, Razansky D. Volumetric real-time tracking of peripheral human vasculature with GPU-accelerated three-dimensional optoacoustic tomography. IEEE Trans Med Imaging 2013;32:2050–5.
32. Niederhauser JJ, Jaeger M, Lemor R, Weber P, Frenz M. Combined ultrasound and optoacoustic system for real-time high-contrast vascular imaging *in vivo*. IEEE Trans Med Imaging 2005;24:436–40.
33. Kolkman RGM, Brands PJ, Steenbergen W, van Leeuwen TG. Real-time *in vivo* photoacoustic and ultrasound imaging. J Biomed Opt 2008;13: 050510.
34. Park S, Karpiouk AB, Aglyamov SR, Emelianov SY. Adaptive beamforming for photoacoustic imaging. Opt Lett 2008;33:1291–3.
35. Fronheiser MP, Ermilov SA, Brecht H-P, Conjusteau A, Su R, Mehta K, et al. Real-time optoacoustic monitoring and three-dimensional mapping of a human arm vasculature. J Biomed Opt 2010;15:021305.
36. Kim C, Erpelding TN, Jankovic L, Wang LV. Performance benchmarks of an array-based hand-held photoacoustic probe adapted from a clinical ultrasound system for non-invasive sentinel lymph node imaging. Philos Transact A Math Phys Eng Sci 2011;369:4644–50.
37. Daoudi K, van den Berg PJ, Rabot O, Kohl A, Tisserand S, Brands P, et al. Handheld probe integrating laser diode and ultrasound transducer array for ultrasound/photoacoustic dual modality imaging. Opt Express 2014; 22:26365.
38. Taruttis A, Morscher S, Burton NC, Razansky D, Ntziachristos V. Fast multispectral optoacoustic tomography (MSOT) for dynamic imaging of pharmacokinetics and biodistribution in multiple organs. PloS One 2012;7:e30491.
39. Morscher S, Driessen WHP, Claussen J, Burton NC. Semi-quantitative Multispectral Optoacoustic Tomography (MSOT) for volumetric PK imaging of gastric emptying. Photoacoustics 2014;2:103–10.
40. Ho CJH, Balasundaram G, Driessen W, McLaren R, Wong CL, Dinish US, et al. Multifunctional photosensitizer-based contrast agents for photoacoustic imaging. Sci Rep 2014;4:5342.
41. Taruttis A, Rosenthal A, Kacprowicz M, Burton NC, Ntziachristos V. Multi-scale multispectral optoacoustic tomography by a stationary wavelet transform prior to unmixing. IEEE Trans Med Imaging 2014;33: 1194–1202.
42. Laufer J, Johnson P, Zhang E, Treeby B, Cox B, Pedley B, et al. *In vivo* preclinical photoacoustic imaging of tumor vasculature development and therapy. J Biomed Opt 2012;17:056016.
43. Li M-L, Oh J-T, Xie X, Ku G, Wang W, Li C, et al. Simultaneous molecular and hypoxia imaging of brain tumors *in vivo* using spectroscopic photoacoustic tomography. Proc IEEE 2008;96:481–9.
44. Heijblom M, Klaase JM, van den Engh FM, van Leeuwen TG, Steenbergen W, Manohar S. Imaging tumor vascularization for detection and diagnosis of breast cancer. Technol Cancer Res Treat 2011;10:607–23.
45. Fatakdawala H, Poti S, Zhou F, Sun Y, Bec J, Liu J, et al. Multimodal *in vivo* imaging of oral cancer using fluorescence lifetime, photoacoustic and ultrasound techniques. Biomed Opt Express 2013;4:1724–41.
46. Dogra VS, Chinni BK, Valluru KS, Joseph JV, Ghazi A, Yao JL, et al. Multispectral photoacoustic imaging of prostate cancer: preliminary *ex-vivo* results. J Clin Imaging Sci 2013;3:41.
47. Needles A, Heinmiller A, Sun J, Theodoropoulos C, Bates D, Hirson D, et al. Development and initial application of a fully integrated photoacoustic micro-ultrasound system. IEEE Trans Ultrason Ferroelectr Freq Control 2013;60:888–97.
48. Ruan Q, Xi L, Boye SL, Han S, Chen ZJ, Hauswirth WW, et al. Development of an anti-angiogenic therapeutic model combining scAAV2-delivered siRNAs and noninvasive photoacoustic imaging of tumor vasculature development. Cancer Lett 2013;332:120–9.

49. Grootendorst DJ, Jose J, Wouters MW, van Boven H, Van der Hage J, Van Leeuwen TG, et al. First experiences of photoacoustic imaging for detection of melanoma metastases in resected human lymph nodes. Lasers Surg Med 2012;44:541–9.
50. Langhout GC, Grootendorst DJ, Nieweg OE, Wouters MWJM, van der Hage JA, Jose J, et al. Detection of melanoma metastases in resected human lymph nodes by noninvasive multispectral photoacoustic imaging. Int J Biomed Imaging 2014;2014:163652.
51. Galanzha EI, Shashkov EV, Spring PM, Suen JY, Zharov VP. *In vivo*, noninvasive, label-free detection and eradication of circulating metastatic melanoma cells using two-color photoacoustic flow cytometry with a diode laser. Cancer Res 2009;69:7926–34.
52. Jansen K, van der Steen AFW, Wu M, van Beusekom HMM, Springeling G, Li X, et al. Spectroscopic intravascular photoacoustic imaging of lipids in atherosclerosis. J Biomed Opt 2014;19:026006.
53. Wang B, Karpiouk A, Yeager D, Amirian J, Litovsky S, Smalling R, et al. *In vivo* intravascular ultrasound-guided photoacoustic imaging of lipid in plaques using an animal model of atherosclerosis. Ultrasound Med Biol 2012;38:2098–2103.
54. Xu Z, Li C, Wang LV. Photoacoustic tomography of water in phantoms and tissue. J Biomed Opt 2010;15:036019.
55. Zhou Y, Zhang C, Yao D-K, Wang LV. Photoacoustic microscopy of bilirubin in tissue phantoms. J Biomed Opt 2012;17:126019.
56. Zhang C, Zhang YS, Yao D-K, Xia Y, Wang LV. Label-free photoacoustic microscopy of cytochromes. J Biomed Opt 2013;18:20504.
57. Yao D-K, Maslov K, Shung KK, Zhou Q, Wang LV. *In vivo* label-free photoacoustic microscopy of cell nuclei by excitation of DNA and RNA. Opt Lett 2010;35:4139–41.
58. Kim C, Song KH, Gao F, Wang LV. Sentinel lymph nodes and lymphatic vessels: noninvasive dual-modality *in vivo* mapping by using indocyanine green in rats—volumetric spectroscopic photoacoustic imaging and planar fluorescence imaging. Radiology 2010;255:442–50.
59. Hellebust A, Richards-Kortum R. Advances in molecular imaging: targeted optical contrast agents for cancer diagnostics. Nanomed 2012;7:429–45.
60. Levi J, Kothapalli S-R, Bohndiek S, Yoon J-K, Dragulescu-Andrasi A, Nielsen C, et al. Molecular photoacoustic imaging of follicular thyroid carcinoma. Clin Cancer Res 2013;19:1494–1502.
61. Wu W, Driessen W, Jiang X. Oligo(ethylene glycol)-based thermosensitive dendrimers and their tumor accumulation and penetration. J Am Chem Soc 2014;136:3145–55.
62. Eghtedari M, Oraevsky A, Copland JA, Kotov NA, Conjusteau A, Motamedi M. High sensitivity of *in vivo* detection of gold nanorods using a laser optoacoustic imaging system. Nano Lett 2007;7:1914–8.
63. Mallidi S, Larson T, Tam J, Joshi PP, Karpiouk A, Sokolov K, et al. Multiwavelength photoacoustic imaging and plasmon resonance coupling of gold nanoparticles for selective detection of cancer. Nano Lett 2009;9:2825–31.
64. Kircher MF, de la Zerda A, Jokerst JV, Zavaleta CL, Kempen PJ, Mittra E, et al. A brain tumor molecular imaging strategy using a new triple-modality MRI-photoacoustic-Raman nanoparticle. Nat Med 2012;18:829–34.
65. Homan KA, Souza M, Truby R, Luke GP, Green C, Vreeland E, et al. Silver nanoplate contrast agents for *in vivo* molecular photoacoustic imaging. ACS Nano 2012;6:641–50.
66. Wilson K, Homan K, Emelianov S. Biomedical photoacoustics beyond thermal expansion using triggered nanodroplet vaporization for contrast-enhanced imaging. Nat Commun 2012;3:618.
67. De la Zerda A, Zavaleta C, Keren S, Vaithilingam S, Bodapati S, Liu Z, et al. Carbon nanotubes as photoacoustic molecular imaging agents in living mice. Nat Nanotechnol 2008;3:557–62.
68. Yang K, Zhu L, Nie L, Sun X, Cheng L, Wu C, et al. Visualization of protease activity *in vivo* using an activatable photo-acoustic imaging probe based on CuS nanoparticles. Theranostics, 2014;4:134–41.
69. Grootendorst DJ, Fratila RM, Visscher M, Haken BT, van Wezel RJA, Rottenberg S, et al. Intra-operative *ex vivo* photoacoustic nodal staging in a rat model using a clinical superparamagnetic iron oxide nanoparticle dispersion. J Biophotonics 2013;6:493–504.
70. Xi L, Satpathy M, Zhao Q, Qian W, Yang L, Jiang H. HER-2/neu targeted delivery of a nanoprobe enables dual photoacoustic and fluorescence tomography of ovarian cancer. Nanomedicine Nanotechnol Biol Med 2013;10:669–77.
71. Deliolanis NC, Ale A, Morscher S, Burton NC, Schaefer K, Radrich K, et al. Deep-tissue reporter-gene imaging with fluorescence and optoacoustic tomography: a performance overview. Mol Imaging Biol 2014;16:652–60.
72. Krumholz A, Shcherbakova DM, Xia J, Wang LV, Verkhusha VV. Multi-contrast photoacoustic *in vivo* imaging using near-infrared fluorescent proteins. Sci Rep 2014;4:3939.
73. Paproski RJ, Heinmiller A, Wachowicz K, Zemp RJ. Multi-wavelength photoacoustic imaging of inducible tyrosinase reporter gene expression in xenograft tumors. Sci Rep 2014;4:5329.
74. Stritzker J, Kirscher L, Scadeng M, Deliolanis NC, Morscher S, Symvoulidis P, et al. Vaccinia virus-mediated melanin production allows MR and optoacoustic deep tissue imaging and laser-induced thermotherapy of cancer. Proc Natl Acad Sci U S A 2013;110:3316–20.
75. Manohar S, Vaartjes SE, van Hespen JCG, Klaase JM, van den Engh FM, Steenbergen W, et al. Initial results of *in vivo* non-invasive cancer imaging in the human breast using near-infrared photoacoustics. Opt Express 2007;15:12277–85.
76. Ermilov SA, Khamapirad T, Conjusteau A, Leonard MH, Lacewell R, Mehta K, et al. Laser optoacoustic imaging system for detection of breast cancer. J Biomed Opt 2009;14:024007.
77. Heijblom M, Piras D, Xia W, van Hespen JCG, Klaase JM, van den Engh FM, et al. Visualizing breast cancer using the Twente photoacoustic mammoscope: what do we learn from twelve new patient measurements? Opt Express 2012;20:11582–97.
78. Berg WA, Gutierrez L, NessAiver MS, Carter WB, Bhargavan M, Lewis RS, et al. Diagnostic accuracy of mammography, clinical examination, US, and MR imaging in preoperative assessment of breast cancer. Radiology 2004;233:830–49.
79. Vionnet L, Gateau J, Schwarz M, Buehler A, Ermolayev V, Ntziachristos V. 24MHz scanner for optoacoustic imaging of skin and burn. IEEE Trans Med Imaging 2013;33:535–45.
80. Favazza CP, Jassim O, Cornelius LA, Wang LV. *In vivo* photoacoustic microscopy of human cutaneous microvasculature and a nevus. J Biomed Opt 2011;16:016015.
81. Yang J-M, Favazza C, Chen R, Yao J, Cai X, Maslov K, et al. Simultaneous functional photoacoustic and ultrasonic endoscopy of internal organs *in vivo*. Nat Med 2012;18:1297–1302.
82. Yang J-M, Chen R, Favazza C, Yao J, Li C, Hu Z, et al. A 2.5-mm diameter probe for photoacoustic and ultrasonic endoscopy. Opt Express 2012;20:23944–53.
83. Karliczek A, Harlaar NJ, Zeebregts CJ, Wiggers T, Baas PC, van Dam GM. Surgeons lack predictive accuracy for anastomotic leakage in gastrointestinal surgery. Int J Colorectal Dis 2009;24:569–76.
84. Schaafsma BE, Mieog JS, Hutteman M, van der Vorst JR, Kuppen PJ, Lowik CW, et al. The clinical use of indocyanine green as a near-infrared fluorescent contrast agent for image-guided oncologic surgery. J Surg Oncol 2011;104:323–32.
85. Song KH, Kim C, Cobley CM, Xia Y, Wang LV. Near-infrared gold nanocages as a new class of tracers for photoacoustic sentinel lymph node mapping on a rat model. Nano Lett 2009;9:183–8.
86. Erpelding TN, Kim C, Pramanik M, Jankovic L, Maslov K, Guo Z, et al. Sentinel lymph nodes in the rat: noninvasive photoacoustic and US imaging with a clinical US system. Radiology 2010;256:102–10.
87. Jose J, Grootendorst DJ, Vijn TW, Wouters MW, Wouters M, van Boven H, et al. Initial results of imaging melanoma metastasis in resected human lymph nodes using photoacoustic computed tomography. J Biomed Opt 2011;16:096021.
88. Xi L, Zhou G, Gao N, Yang L, Gonzalo DA, Hughes SJ, et al. Photoacoustic and fluorescence image-guided surgery using a multifunctional targeted nanoprobe. Ann Surg Oncol 2014;21:1602–9.
89. Sturm MB, Joshi BP, Lu S, Piraka C, Khondee S, Elmunzer BJ, et al. Targeted imaging of esophageal neoplasia with a fluorescently labeled peptide: first-in-human results. Sci Transl Med 2013;5:184ra61.
90. Hsiung P, Hardy J, Friedland S, Soetikno R, Du CB, Wu AP, et al. Detection of colonic dysplasia *in vivo* using a targeted fluorescent septapeptide and confocal microendoscopy. Nat Med 2008;14:454–8.
91. Cox B, Laufer JG, Arridge SR, Beard PC. Quantitative spectroscopic photoacoustic imaging: a review. J Biomed Opt 2012;17:061202.